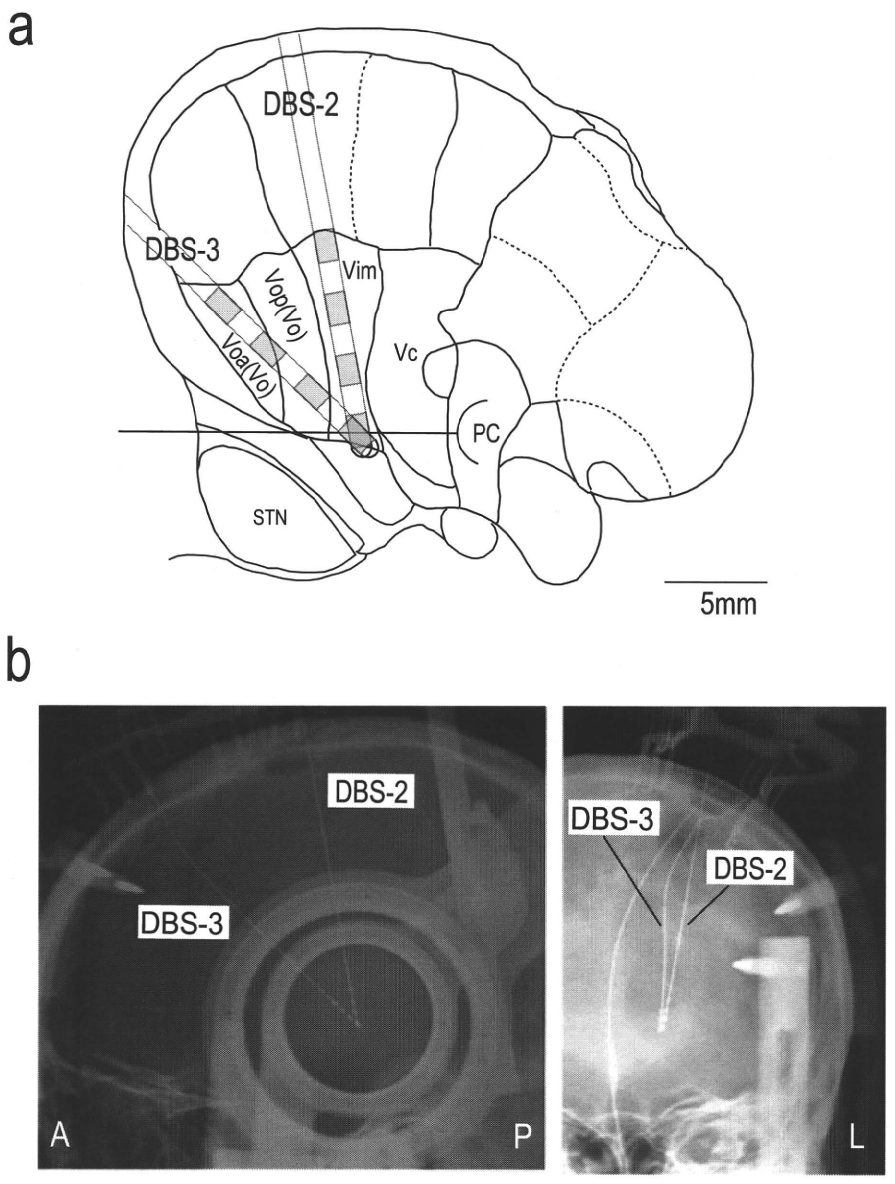

FIGURE 2. Intraoperative radiographs and anatomic relationship between thalamic nucleus and deep brain stimulation (DBS) electrode. (a) The 14.5-mm lateral section from the Schaltenbrand–Wahren human brain atlas with the anterior commissure–posterior commissure (AC–PC) length is stretched to fit the coordinates obtained from the patient's stereotactic magnetic resonance imaging. DBS-2, the second electrode of DBS, was temporarily implanted at a high angle to the AC–PC line. DBS-3, the third electrode of DBS, was placed at a low angle to the AC–PC line. PC, posterior commissure; STN, subthalamic nucleus; Vc, nucleus ventrocaudalis; Vim, nucleus ventralis intermedius; Vo, nucleus ventralis oralis; Voa, nucleus ventralis oralis anterior; Vop, nucleus ventralis oralis posterior. (b) Two radiographs are superimposed, each of which was obtained when the DBS electrode was inserted along a different trajectory. The labels DBS-2 and DBS-3 indicate DBS-2 and DBS-3 shown on the brain map in a, respectively. Left, lateral view; Right, anterior-posterior view.

Because the Vim forms an oblong structure on the lateral view, the DBS electrode must be inserted at a high angle to the horizontal plane of the AC–PC line, thereby allowing the contacts of the electrode to be arranged in the Vim as much as possible. However, in our patient, despite arranging the four contacts of the first and second DBS electrodes in the Vim, his tremor was not affected. The target for the third DBS electrode was approached at an angle of 45° to

the horizontal plane of the AC–PC line. This trajectory produced a microthalamotomy effect even though the target was nearly the same as that for the second DBS electrode. The main difference in the placement of the second and third DBS electrodes was the trajectory through the thalamus (Fig. 2). However, it is possible that the second DBS electrode was located in the somatotopic area of the Vim corresponding to the lower extremity instead of in the area corresponding to the upper extremity because the second DBS electrode was slightly lateral to the third DBS electrode. That is, contact 0 of the second DBS electrode was approximately 0.5 mm lateral to contact 0 of the third DBS electrode and contact 3 of the second DBS electrode was approximately 1.5 mm lateral to contact 3 of the third DBS electrode (A–P view shown in Fig. 2b). There are few reports on thalamic stimulation therapy for tremor in which the optimal angle of the DBS electrode to the AC–PC line or optimal trajectory through the thalamic regions is reported. However, it was demonstrated that stimulation of both Vim and Vo is necessary in many cases. One study implied that the optimal angle of the DBS electrode to the AC–PC line should be approximately 45° (9). In the large series of cases presented by Benabid et al., (2) the optimal tremor control site was located 4 to 8 mm anterior to the PC, and 0 to 2 mm superior to the AC–PC line. Therefore, with these coordinates, it is possible that the areas affected by the spread of the current stimulation included not only the Vim but also the Vo (23).

Thalamic neurons firing at the same frequency as that of tremor have been recorded during surgery and such neurons are widely distributed over an area extending from the Vim to the Vo (24–28). Some of these neurons are involved in the generation of tremor (24,29). That is, the wide area of the ventral thalamic nuclei may be involved in the generation of tremor. It would therefore be difficult to ablate the extensive area implicated in the generation of tremor without any side-effects. In contrast, DBS electrodes can be implanted to affect an area wider than that affected by thalamotomy, and still allow a surgeon to select a location to place the contacts and modify the stimulation intensity as required, thereby achieving the best clinical benefits (1–3,9,10).

Because of the large angle of the trajectory of the third DBS electrode, there is a possibility of inadvertently making a burr hole in the forehead. In our patient, specific management was not required to maintain an esthetic appearance of the forehead. If we had considered that an accidental of burr hole in the forehead was likely, we would have made a transverse skin incision on the hair line.

Conclusion

We report on a patient who had different effects on tremor depending on the trajectory angle of the DBS electrode to the AC–PC line. The trajectory of the DBS electrode may be a considerable factor for the implantation of a DBS electrode for tremor therapy.

Conflict of Interest

The authors reported no conflict of interest.

References

1. Benabid AL, Pollak P, Gervason C et al. Long-term suppression of tremor by chronic stimulation of the ventral intermediate thalamic nucleus. *Lancet* 1991;337:403–406.

2. Benabid AL, Pollak P, Gao D et al. Chronic electrical stimulation of the ventralis intermedius nucleus of the thalamus as a treatment of movement disorders. *J Neurosurg* 1996;84:203–214.

3. Blond S, Caparros-Lefebvre D, Parker F et al. Control of tremor and involuntary movement disorders by chronic stereotactic stimulation of the ventral intermediate thalamic nucleus. *J Neurosurg* 1992;77:62–68.

4. Caparros-Lefebvre D, Blond S, Vermersch P, Pecheux N, Guieu JD, Petit H. Chronic thalamic stimulation improves tremor and levodopa induced dyskinesias in Parkinson's disease. *J Neurol Neurosurg Psychiatry* 1993;56:268–273.

5. Katayama Y, Fukaya C, Yamamoto T. Control of post-stroke involuntary and voluntary movement disorders with deep brain or epidural cortical stimulation. *Stereotact Funct Neurosurg* 1997;69:73–79.

6. Koller WC, Lyons KE, Wilkinson SB, Troster AI, Pahwa R. Long-term safety and efficacy of unilateral deep brain stimulation of the thalamus in essential tremor. *Mov Disord* 2001;16:464–468.

7. Limousin P, Speelman JD, Gielen F, Janssens M. Multicentre European study of thalamic stimulation in parkinsonian and essential tremor. *J Neurol Neurosurg Psychiatry* 1999;66:289–296.

8. Nguyen JP, Degos JD. Thalamic stimulation and proximal tremor. A specific target in the nucleus ventrointermedius thalami. *Arch Neurol* 1993;50:498–500.

9. Yamamoto T, Katayama Y, Kano T, Kobayashi K, Oshima H, Fukaya C. Deep brain stimulation for the treatment of parkinsonian, essential, and poststroke tremor: a suitable stimulation method and changes in effective stimulation intensity. *J Neurosurg* 2004;101:201–209.

10. Yamamoto T, Katayama Y, Fukaya C, Oshima H, Kasai M, Kobayashi K. New method of deep brain stimulation therapy with two electrodes implanted in parallel and side by side. *J Neurosurg* 2001;95:1075–1078.

11. Nagaseki Y, Shibazaki T, Hirai T et al. Long-term follow-up results of selective VIM-thalamotomy. *J Neurosurg* 1986; 65:296–302.

12. Ohye C, Narabayashi H. Physiological study of presumed ventralis intermedius neurons in the human thalamus. *J Neurosurg* 1979;50:290–297.

13. Lenz FA, Normand SL, Kwan HC et al. Statistical prediction of the optimal site for thalamotomy in parkinsonian tremor. *Mov Disord* 1995;10:318–328.

14. Gabriel EM, Nashold BS Jr. Evolution of neuroablative surgery for involuntary movement disorders: an historical review. *Neurosurgery* 1998;42:575–590; discussion 590–591.

15. Schuurman PR, Bosch DA, Bossuyt PM et al. A comparison of continuous thalamic stimulation and thalamotomy for suppression of severe tremor. *N Engl J Med* 2000;342:461–468.

16. Katayama Y, Kano T, Kobayashi K, Oshima H, Fukaya C, Yamamoto T. Difference in surgical strategies between thalamotomy and thalamic deep brain stimulation for tremor control. *J Neurol* 2005;252 (Suppl. 4):IV17–IV22.

17. Kiss ZH, Wilkinson M, Krcek J et al. Is the target for thalamic deep brain stimulation the same as for thalamotomy? *Mov Disord* 2003;18:1169–1175.

18. Hua SE, Lenz FA. Posture-related oscillations in human cerebellar thalamus in essential tremor are enabled by voluntary motor circuits. *J Neurophysiol* 2005;93:117–127.

19. Tasker RR. Deep brain stimulation is preferable to thalamotomy for tremor suppression. *Surg Neurol* 1998;49:145–153; discussion 153–154.

20. Kondziolka D, Lee JY. Long-lasting microthalamotomy effect after temporary placement of a thalamic stimulating electrode. *Stereotact Funct Neurosurg* 2004;82:127–130.

21. Hirai T, Miyazaki M, Nakajima H, Shibazaki T, Ohye C. The correlation between tremor characteristics and the predicted volume of effective lesions in stereotaxic nucleus ventralis intermedius thalamotomy. *Brain* 1983;106:1001–1018.

22. Lenz FA, Kwan HC, Dostrovsky JO, Tasker RR, Murphy JT, Lenz YE. Single unit analysis of the human ventral thalamic nuclear group. Activity correlated with movement. *Brain* 1990;113: 1795–1821.

23. Starr PA, Vitek JL, Bakay RA. Ablative surgery and deep brain stimulation for Parkinson's disease. *Neurosurgery* 1998;43: 989–1013; discussion 1013–1015.

24. Lenz FA, Kwan HC, Martin RL, Tasker RR, Dostrovsky JO, Lenz YE. Single unit analysis of the human ventral thalamic nuclear group. Tremor-related activity in functionally identified cells. *Brain* 1994;117:531–543.

25. Zirh TA, Lenz FA, Reich SG, Dougherty PM. Patterns of bursting occurring in thalamic cells during parkinsonian tremor. *Neuroscience* 1998;83:107–121.

26. Lenz FA, Jaeger CJ, Seike MS, Lin YC, Reich SG. Single-neuron analysis of human thalamus in patients with intention tremor and other clinical signs of cerebellar disease. *J Neurophysiol* 2002;87:2084–2094.

27. Kobayashi K, Katayama Y, Kasai M, Oshima H, Fukaya C, Yamamoto T. Localization of thalamic cells with tremor-frequency activity in Parkinson's disease and essential tremor. *Acta Neurochir Suppl* 2003;87:137–139.

28. Brodkey JA, Tasker RR, Hamani C, McAndrews MP, Dostrovsky JO, Lozano AM. Tremor cells in the human thalamus: differences among neurological disorders. *J Neurosurg* 2004;101: 43–47.

29. Lenz FA, Tasker RR, Kwan HC et al. Single unit analysis of the human ventral thalamic nuclear group: correlation of thalamic "tremor cells" with the 3–6 Hz component of parkinsonian tremor. *J Neurosci* 1988;8:754–764.

Comments

This is an interesting case report that highlights the importance of the angle of approach in deep brain stimulation (DBS) surgeries. The trajectory and the angle of implantation dictates the final location of the DBS within the various structures and influences the benefits and side effects. The authors show in this one case that a more anterior and shallow angle of approach encompassing the VOP/VIM target has better efficacy than a posterior and vertical approach to the VIM. Additional studies are needed to further investigate this concept.

Ali R. Rezai, MD
Julius F. Stone Endowed Chair
Professor of Neurosurgery
Director, OSU Center for Neuromodulation
Director, Functional Neurosurgery
Director, Neurosurgical Innovations
Vice Chair, Neurosurgery Clinical Research
The Ohio State University
Department of Neurological Surgery
Columbus, Ohio USA

This is an interesting paper reporting that changing the angle of trajectory may influence the efficacy of deep brain stimulation. Certainly it reflects my experience with essential tremor in that pure VIM stimulation may not suppress ET effectively. I target the VOP and VIM as much as I can in the approach. Essential tremor is not benign at all, the tremor can become resistant to stimulation in a significant number of patients. I therefore advise my patients with ET to turn the stimulator on only if they need to do a task.

The authors of this paper suggest an extremely shallow angle that straddles VOP and VIM with good effect. I wonder if this might in some cases cause an unsightly forehead scar. Nevertheless this is an interesting case report.

Tipu Aziz, MD, MBBS, FRCS
Professor
Neurosurgery Department
John Radcliffe Hospital
Oxford University
Oxford, United Kingdom

Clinical Study

Stereotactic and Functional Neurosurgery

Stereotact Funct Neurosurg 2010;88:163–168
DOI: 10.1159/000313868

Received: July 27, 2009
Accepted after revision: February 25, 2010
Published online: May 1, 2010

Nexframe Frameless Stereotaxy with Multitract Microrecording: Accuracy Evaluated by Frame-Based Stereotactic X-Ray

Chikashi Fukaya[a, b] Koichiro Sumi[a, b] Toshiharu Otaka[a, b] Toshiki Obuchi[a, b] Toshikazu Kano[a, b] Kazutaka Kobayashi[a, b] Hideki Oshima[a–c] Takamitsu Yamamoto[a, b] Yoichi Katayama[a, b]

[a]Division of Applied System Neuroscience, Advanced Medical Research Center, and Departments of [b]Neurological Surgery and [c]Functional Morphology, Nihon University School of Medicine, Tokyo, Japan

Key Words
Frameless stereotaxy · Multitract microrecording · Deep brain stimulation · Parkinson's disease · Subthalamic nucleus

Abstract
Objective: The development of image-guided systems rendered it possible to perform frameless stereotactic surgery for deep brain stimulation (DBS). As well as stereotactic targeting, neurophysiological identification of the target is important. Multitract microrecording is an effective technique to identify the best placement of an electrode. This is a report of our experience of using the Nexframe frameless stereotaxy with Ben's Gun multitract microrecording drive and our study of the accuracy, usefulness and disadvantages of the system. ***Methods:*** Five patients scheduled to undergo bilateral subthalamic nucleus (STN) DBS were examined. The Nexframe device was adjusted to the planned target, and electrodes were introduced using a microdrive for multitract microrecording. In addition to the Nexframe frameless system, we adopted the Leksell G frame to the same patients simultaneously to use a stereotactic X-ray system. This system consisted of a movable X-ray camera with a crossbar and was adopted to be always parallel to the frame with the X-ray film cassette. The distance between the expected and actual DBS electrode placements was measured on such a stereotactic X-ray system. In addition, the distance measured with this system was compared with that measured by conventional frame-based stereotaxy in 20 patients (40 sides). ***Results:*** The mean deviations from 10 planned targets were 1.3 ± 0.3 mm in the mediolateral (x) direction, 1.0 ± 0.9 mm in the anteroposterior (y) direction and 0.5 ± 0.6 mm in the superoposterior (z) direction. The data from the frame-based stereotaxy in our institute were 1.5 ± 0.9 mm in the mediolateral (x) direction, 1.1 ± 0.7 mm in the anteroposterior (y) direction and 0.8 ± 0.6 mm in the superoposterior (z) direction. Then, differences were not statistically significant in any direction ($p > 0.05$). The multitract microrecording procedure associated with the Nexframe was performed without any problems in all of the patients. None of these electrodes migrated during and/or after the surgery. However, the disadvantage of the system is the narrow surgical field for multiple electrode insertion. Coagulating the cortex and inserting multiple electrodes under such a narrow visual field were complicated. ***Conclusion:*** The Nexframe with multitract microrecording for STN DBS still has some problems that need to be resolved. Thus far, we do not consider that this technology in its present state can replace conventional frame-based stereotactic surgery. The accuracy of the system is similar to that of frame-based stereotaxy. However, the narrow surgical field is a disadvantage for multiple electrode insertion. Improvement on this point will enhance the usefulness of the system.

KARGER

Fax +41 61 306 12 34
E-Mail karger@karger.ch
www.karger.com

1011–6125/10/0883–0163$26.00/0

Accessible online at:
www.karger.com/sfn

Hideki Oshima, MD, PhD
Department of Neurological Surgery
Nihon University School of Medicine
30-1, Ohyaguchi Kamimachi, Itabashi-ku, Tokyo 173-8610 (Japan)
Tel. +81 3 3972 8111, Fax +81 3 3554 0425, E-Mail chikashi@med.nihon-u.ac.jp

Introduction

Deep brain stimulation (DBS) has been shown to be an effective treatment for medically refractory functional neurological diseases such as movement disorders and intractable pain. Neurosurgical interventions for DBS are conventionally performed with the aid of the frame-based stereotactic procedure. Since the introduction of stereotactic functional neurosurgery, this method has been the standard for stereotactic surgical procedures including the implantation of DBS electrodes.

Application of a stereotactic frame throughout a lengthy procedure often plunges a patient into an uncomfortable feeling. The development of techniques for image-guided neurosurgical systems rendered it possible to perform stereotactic brain surgery without a conventional frame fixed to the skull bone [1–3].

The exact placement of a DBS electrode in the target is a crucial step to maximize the benefits and avoid side effects of stimulation. As well as the stereotactic targeting based on MRI, neurophysiological identification of the target is an important procedure. Multitract microrecording is an effective method to identify the best placement of electrodes [4]. The system is becoming increasingly popular as a standard technique for stereotactic DBS electrode implantation.

We report our experience of using the new surgical technique of Nexframe frameless stereotaxy coupled with the multitract microrecording system. The present study was also conducted to evaluate the accuracy, usefulness and disadvantages of this system used for the treatment of Parkinson's disease (PD) with subthalamic nucleus (STN) stimulation.

To evaluate the accuracy of this system, we used a frame-based stereotactic X-ray system that makes it possible to assess the electrode position in both anteroposterior and lateral directions. Unlike MRI, electrode position designated by X-ray imaging reveals a precise coordination unaffected by a bias caused by an artifact on images. We calculated the deviations of electrode position from the planned target on such a stereotactic X-ray system. These deviations were compared with the data of patients who underwent frame-based stereotactic surgery in our institute during the same period.

Clinical Materials and Methods

The clinical materials were 5 patients who had PD with bilateral symptoms and were scheduled to undergo bilateral STN DBS. Three patients were male and 2 were female. The mean age ± standard deviation (SD) was 63.2 ± 5.6 years, and the disease duration was in the range of 7–14 years (10.6 ± 2.9 years). All of the patients gave their informed consent in writing. They were clearly informed that an electrode would be replaced during the same operation using the routine frame-based technique if it was not adequately placed using the frameless system.

We used a Nexframe frameless stereotactic system (Image-Guided Neurologics, Melbourne, Fla., USA), and the targeting was guided using a Stealth Treon neuronavigation system (Medtronic, SNT, Louisville, Colo., USA). The data of single- and multiunit extracellular action potentials were collected using Framelink v. 4.1 software (Medtronic, Minneapolis, Minn., USA) together with a Ben's Gun multitract microrecording device (FHC drive, Frederick Haer Corporation, Brunswick, Me., USA).

In addition to these devices, we used a frame-based stereotactic X-ray system (Elekta-Fujita Ika Kogyo, Tokyo, Japan) to evaluate the precise electrode position. This system consisted of a movable X-ray camera with a crossbar and was adopted to be always parallel to the frame with the X-ray film cassette (fig. 1). In the anterior and lateral positions, the central X-ray beam is supposed to pass through the center of the frame. This stereotactic X-ray system has already been approved by the Japanese government for its accuracy and safety as medical equipment and is commercially available only in Japan. To use this system, the Leksell G frame (Elekta AB, Stockholm, Sweden) was adopted in the same patients simultaneously.

The day prior to surgery, 6 bone fiducial markers were screwed into the skull bone after application of a local anesthetic agent. CT slices showing the fiducial markers were exported to Stealth Treon for fusing with MRI, which were used for registration of the frameless neuronavigation system. The Leksell G frame was fixed to the skull before MRI in the operative room. MRI (Magnetom Symphony, 1.5-tesla scanner, Siemens, Erlangen, Germany) was used for targeting, and the sequences of MRI were 3-dimensional volumetric T_1-weighted 1-mm slices, inversion recovery fast-field echo and 2-mm T_2-weighted MRI slices in axial projections.

MR and CT images were exported in the Dicom format to the Stealth Treon neuronavigation system for target planning. Target and trajectories were planned from entry points at the suitable gyrus without passing the ventricular walls. Following the making of entry points on the scalp, burr holes were formed after local anesthesia injection. After these procedures, the Nexframe was fixed on the frontal skull, and a sterile reference arc was fastened to the base of the Nexframe.

The Nexframe was adjusted to the planned target, and a cannula with a blunt mandrel was introduced using the drive for multitract microrecording (fig. 2). We used 3 trajectories for microrecording of each side. In all of the patients, cannulas were introduced into the central, lateral and posterior positions of the multitract microdrive. The coordinate for a tentative target was applied to the electrode in the central position. Microrecording was performed 10 mm above the tentative target. On the basis of intraoperative neurophysiological findings and the results of macrostimulation during the surgery, we finally decided on the tract into which a DBS electrode would be implanted (model 3387; Medtronic, Minneapolis, Minn., USA) persistently. Following the implantation of the quadripolar DBS electrode, stereotactic X-ray images from the frontal and lateral projections were obtained.

We carried out the surgical procedure for electrode implantation basically employing the C arm, which is the standard proce-

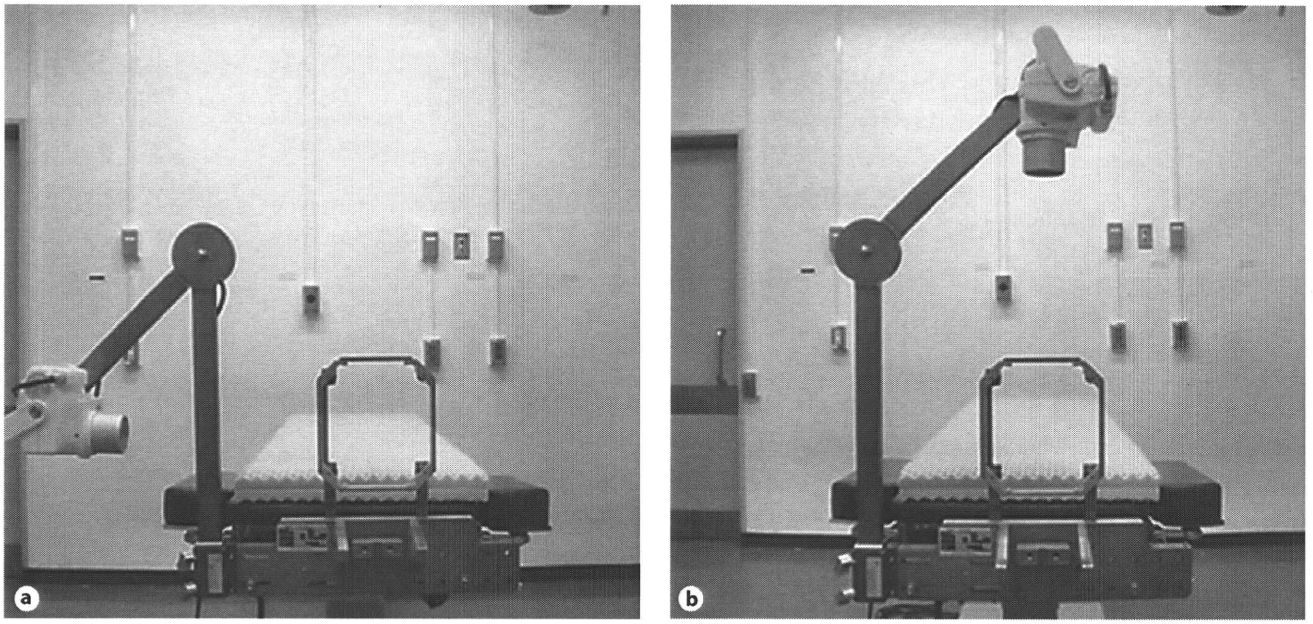

Fig. 1. The stereotactic X-ray system used in this study consisted of a movable X-ray camera with a crossbar and was adopted to be always parallel to the frame with the X-ray film cassette. **a** Stereotactic X-ray system for the evaluation from lateral projection. **b** Lower setting from anterior-posterior projections.

dure for the Nexframe frameless system. The final confirmation of the electrode position was achieved using the frame-based stereotactic X-ray system. The distance between the planned target and the actual DBS electrode position was measured on stereotactic X-ray images. Electrode location was documented in anterior commissure/posterior commissure (AC-PC) coordinates as a signed distance in each of the x-, y- and z-coordinates.

Immediately following surgery, CT images were obtained to assess postoperative hemorrhage and other surgical complications. Also, the final electrode location could be crudely evaluated from the center of the artifact representing the deepest electrode. However, since the center of the artifact was sometimes not evident on CT images, stereotactic X-ray imaging was preferentially taken into consideration as an appropriate method for analysis in this study.

The expected distance and actual location were compared with the data collected during the frame-based stereotactic surgery using the Leksell G frame. The data were collected from 20 patients who underwent STN DBS using the standard frame-based technique in our institute during the same 6 months when we performed STN DBS using the frameless technique (June to November 2008). The distance was calculated similarly to when using the stereotactic X-ray system. We used the unpaired Student's t test for statistical analysis.

The study protocol was approved by our Institutional Review Board, and written informed consent was obtained from all of the patients prior to their participation in the study. Patients who chose not to participate had the option of undergoing the standard frame-based stereotactic surgery.

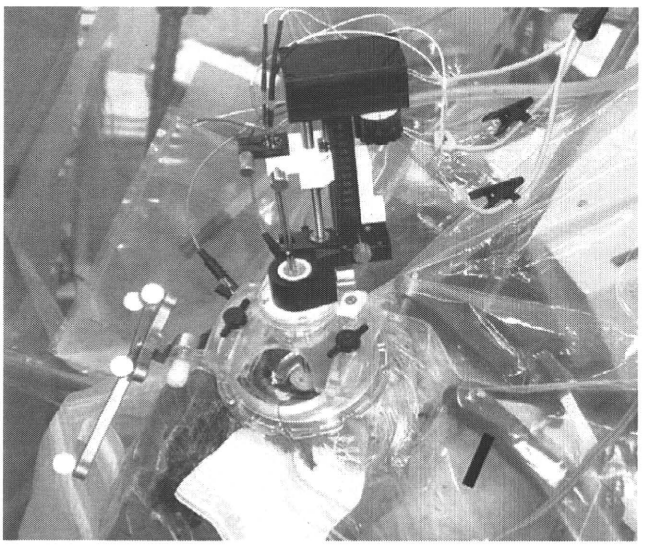

Fig. 2. The Nexframe device was adjusted to the planned target, and microelectrodes were introduced following cannula insertion. Microelectrodes were connected to a Leadpoint system, and recordings were carried out in 3 trajectories simultaneously using a microdrive for multitract microrecording.

Table 1. The deviations from planned targets to real electrode position in the central trajectory (means ± SD and ranges in parentheses, mm)

	Mediolateral (x)	Anteroposterior (y)	Superoposterior (z)
Frameless (n = 10)	1.3 ± 0.3 (0.7–1.9)	1.0 ± 0.9 (0.2–3.4)	0.5 ± 0.6 (0.2–2.1)
Frame-based (n = 40)	1.5 ± 0.9 (0.0–3.5)	1.1 ± 0.7 (0.2–3.4)	0.8 ± 0.6 (0.0–2.4)
p value	0.36	0.69	0.21

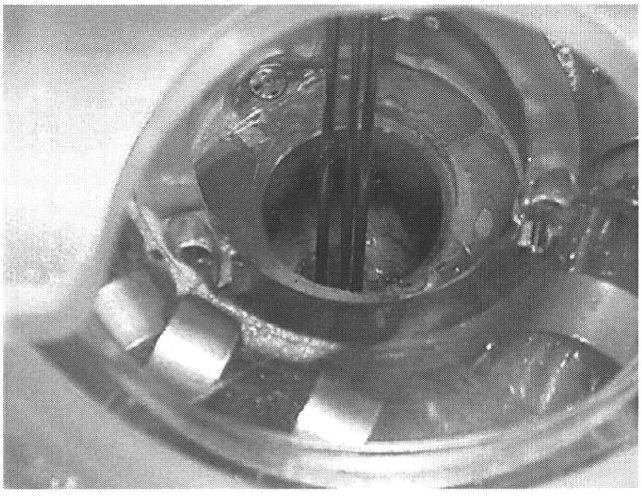

Fig. 3. The technical inconvenience of this system was due to the narrow surgical field for the insertion of multiple electrodes with the cannula for multitract microrecording. Particularly in the case of a brain sink, the identification and coagulation of the insertion points on the cortex were complicated, as shown in the figure.

Results

A total of 10 electrodes were implanted in 5 patients using the Nexframe frameless system with the aid of multitract microrecording. No complications, such as infection, intracranial hemorrhage or skin erosion, were encountered. None of these electrodes moved or migrated during and/or after the surgery.

Tentative targets were set as the tip of the electrode located at the ventral border of the STN. The coordinates of the tentative targets for 10 electrodes were set at (mean ± SD) 12.7 ± 0.8 mm lateral from the midline, 5.6 ± 1.4 mm posterior to the midcommissure point (MC), and 6.3 ± 1.2 mm inferior to the AC-PC line. The final positions of the 10 electrodes were (mean ± SD) 11.3 ± 0.3 mm lateral from the midline, 5.0 ± 0.7 mm posterior to the MC and 5.7 ± 0.4 mm inferior to the AC-PC line.

As shown in table 1, the deviations from the 10 planned targets were (mean ± SD) 1.3 ± 0.3 mm in the mediolateral (x), 1.0 ± 0.9 mm in the anteroposterior (y) and 0.5 ± 0.6 mm in the superoposterior (z) directions. The deviations in the frame-based surgery of 20 patients (40 electrodes) in our institute were (mean ± SD) 1.5 ± 0.9 mm in the mediolateral (x), 1.1 ± 0.7 mm in the anteroposterior (y) and 0.8 ± 0.6 mm in the superoposterior (z) directions. Differences were not statistically significant in any direction between these two groups of patients ($p < 0.05$).

The DBS electrodes were implanted in the central trajectory in 4 of 10 implantations. The trajectories of the remaining electrodes were lateral in 4 and posterior in 2 of the 6 remaining implantations. The multitract microrecording procedure was performed without any complications in all of the patients. Data from the multitract microrecording were obviously useful for identifying the best trajectory for implantation of the DBS electrodes.

However, the technical inconvenience of this system was due to the narrow surgical field during the insertion of electrodes with a cannula for multitract microrecording. In particular, in the case of a brain sink, we found it very difficult to identify and coagulate the insertion points on the cortex (fig. 3). Unlike in frame-based stereotaxy, specifying the electrode insertion points on the cortex is impossible in the Nexframe system. In addition to the narrow surgical field, this disadvantage of the system led to a complex procedure.

All of the patients were eligible for clinical follow-up. Clinical evaluation using UPDRS-2 and -3 at 6 months after the surgery showed a marked improvement in scale. The improvement rate of the UPDRS and the reduction rate of L-dopa equivalent dose were not significantly different statistically between the 5 patients with Nexframe and the 20 patients with frame-based stereotaxy (Mann-Whitney U test).

Discussion

The Nexframe frameless system has recently been introduced by Henderson and his colleagues [1–3]. Their several studies based on a laboratory phantom and/or clinical experience have already proved that the accuracy of the Nexframe device for frameless stereotaxy enables the placement of the DBS electrode at the target coordinate. On the other hand, Bjartmarz and Rehncrona [5] reported that the accuracy for hitting a planned stereotactic target is higher when the conventional frame-based technique is used than when the Nexframe frameless technique is used. They studied the implantation of DBS electrodes in 14 patients with essential tremor. In their study, DBS electrodes were implanted in the ventrolateral thalamus (ventrointermediate nucleus) using the Nexframe on one side and conventional stereotaxy on the other. The exact positions of both electrodes were documented by conventional stereotactic X-ray imaging following the implantation.

We studied the accuracy of Nexframe frameless stereotaxy on 10 sides of the STN in 5 patients with PD using the stereotactic X-ray system. The sample size of our study is not sufficiently large. Therefore, it is difficult to evaluate the statistical significance of the accuracy of the measurements. However, we did not conduct any further investigation because this system is inconvenient and the accuracy of the Nexframe itself was already confirmed by previous studies [1–3]. In addition, it could be presumed that there are some other factors that often lead to errors in the precise placement of the electrode in the STN, including MR image distortion [6], brain shift [7–9] caused by CSF leakage, and air influx. In particular, brain shift almost always occurs after the dura has been opened during surgery and decreases the reliability of precise electrode placement at the target.

Zonenshayn et al. [10] reported that the average distance error between the final physiological targets and the MRI-derived target was 2.6 ± 1.3 mm. Andrade-Souza et al. [11] also reported that the mean distances between the optimal contact position and the planned image-guided target were 3.19 ± 1.19 mm for the red-nucleus-based method, 3.42 ± 1.34 mm for indirect targeting and 4.66 ± 1.33 mm for a modified direct targeting. In addition to these reports, from the study of 50 patients in our institute [9], the MC shifted mainly in the posterior direction (y-axis: 1.27 ± 0.7 mm), and shifts in the inferior direction (z-axis: 0.11 ± 0.43 mm) and lateral direction (x-axis: 0.02 ± 0.39 mm) were noted during the surgery. From these reports, it should be kept in mind to consider the difference between the optimal location and the target coordinate planned by preoperative MRI.

In this study, trajectories except the center were selected in more than 50% of the implantations as the final DBS electrode position. Hence, we should consider that confirmation by microrecording plays an important role as an integral part of stereotactic functional surgical procedures. Recently, multitract microrecording has become increasingly popular as a standard technique for neurophysiological identification of the target, particularly in STN surgery. We believe that the DBS effect can be maximized by applying multitract microrecording.

The configuration of the STN is represented by multitract microrecording, and the longest trajectory with neuronal activity characteristic of the STN can be chosen as the part for chronic stimulation. Being coupled with such a technique, the Nexframe frameless system increases its usefulness and might meet what is achievable by conventional frame-based stereotactic surgery. Eljamel et al. [12] developed a new simple frameless stereotactic device that enabled microrecording in multitracts. However, this device is so far not commercially available.

We reported the first experience of performing the Nexframe frameless procedure along with a Ben's Gun multitract microrecording system. The results of our study show that the accuracy of hitting a planned target using this technique is nearly the same as that using the conventional frame-based technique and we did not encounter any technical problems due to the devices during the surgery. Basically, the accuracy and usefulness of these devices are reliable. However, the disadvantage of this system is the narrow surgical field for electrode insertion to the cortex.

The Nexframe with single-tract recording, which was previously reported, seemed to have the same problem. However, in the case of single-tract recording, coagulation of the cortex for the insertion of 1 electrode is possible without much difficulty. Unlike that case, it was complicated to identify the insertion points and coagulate the cortices in the case of multielectrode insertion in such a narrow surgical field. Such a disadvantage of the Nexframe with multitract microrecording was difficult to evaluate quantitatively in this study. We consider that this is an important issue to be solved in order to use the Nexframe along with the multitract microrecording system easily.

Conclusion

The Nexframe with multitract microrecording for STN DBS still has some problems that need to be resolved. Thus far, we do not consider that this technology in its present state can replace conventional frame-based stereotactic surgery. The accuracy of this system is similar to that of frame-based stereotaxy. However, the narrow surgical field is a disadvantage for multielectrode insertion. Improvement on this point will enhance the usefulness of this system.

References

1 Henderson JM: Frameless localization for functional neurosurgical procedures: a preliminary accuracy study. Stereotact Funct Neurosurg 2004;82:135–141.

2 Henderson JM, Holloway KL, Gaede SE, Rosenow JM: The application accuracy of a skull-mounted trajectory guide system for image-guided functional neurosurgery. Comput Aided Surg 2004;9:155–160.

3 Holloway KL, Gaede SE, Starr PA, Rosenow JM, Ramakrishnan V, Henderson JM: Frameless stereotaxy using bone fiducial markers for deep brain stimulation. J Neurosurg 2005;103:404–413.

4 Tamma F, Caputo E, Chiesa V, Egidi M, Locatelli M, Rampini P, Cinnante C, Pesenti A, Priori A: Anatomo-clinical correlation of intraoperative stimulation-induced side-effects during HF-DBS of the subthalamic nucleus. Neurol Sci 2002;23(suppl 2):S109–S110.

5 Bjartmarz H, Rehncrona S: Comparison of accuracy and precision between frame-based and frameless stereotactic navigation for deep brain stimulation electrode implantation. Stereotact Funct Neurosurg 2007;85:235–242.

6 Bourgeois G, Magnin M, Morel A, Sartoretti S, Huisman T, Tuncdogan E, Meier D, Jeanmonod D: Accuracy of MRI-guided stereotactic thalamic functional neurosurgery. Neuroradiology 1999;41:636–645.

7 Wester K, Krakenes J: Vertical displacement of the brain and the target area during open stereotaxic neurosurgery. Acta Neurochirur (Wien) 2001;143:603–606.

8 Winkler D, Tittgemeyer M, Schwarz J, Preul C, Strecker K, Meixensberger J: The first evaluation of brain shift during functional neurosurgery by deformation field analysis. J Neurol Neurosurg Psychiatry 2005;76:1161–1163.

9 Obuchi T, Katayama Y, Kobayashi K, Oshima H, Fukaya C, Yamamoto T: Direction and predictive factors for the shift of brain structure during deep brain stimulation electrode implantation for advanced Parkinson's disease. Neuromodulation 2008;11:302–310.

10 Zonenshayn M, Rezai AR, Mogilner AY, Beric A, Sterio D, Kelly PJ: Comparison of anatomic and neurophysiological methods for subthalamic nucleus targeting. Neurosurgery 2000;47:282–292.

11 Andrade-Souza YM, Schwalb JM, Hamani C, Eltahawy H, Hoque T, Saint-Cyr J, Lozano AM: Comparison of three methods of targeting the subthalamic nucleus for chronic stimulation in Parkinson's disease. Neurosurgery 2005;56(suppl 2):360–368.

12 Eljamel MS, Tulley M, Spillane K: A simple stereotactic method for frameless deep brain stimulation. Stereotact Funct Neurosurg. 2007;85:6–10.

Effect of Transient Forebrain Ischemia on Flavoprotein Autofluorescence and the Somatosensory Evoked Potential in the Rat

Takahiro Igarashi, Kaoru Sakatani, Tatsuya Hoshino, Norio Fujiwara, Yoshihiro Murata, Tsuneo Kano, Jun Kojima, Takamitsu Yamamoto, and Yoichi Katayama

Abstract In order to evaluate the effect of cerebral ischemia on the flavoprotein fluorescence (FPF), we compared the changes in the FPF and somatosensory evoked potential (SEP) during transient cerebral ischemia in the rat. We measured the FPF and SEP simultaneously via a cranial window made over the right sensorimotor cortex during the left median nerve stimulation in F344 rats. We compared change in FPF and SEP during cerebral ischemia for 60 min. The rCBF were rapidly recovered after reperfusion. However, the recovery rates of the FPF were significantly faster than those of the SEP after reperfusion. These findings indicate that activity-dependent changes of the FPF do not necessarily correlate with the electrical activity after transient cerebral ischemia.

1 Introduction

Recently, it has been demonstrated that the autofluorescence of flavoproteins is applicable for brain functional imaging in rats [7]. Flavoproteins are involved in the electron transfer system of mitochondria. Neuronal activity increases the intracellular Ca^{2+}, which converts the flavoprotein from the reduced form to the oxidized form. The oxidized flavoprotein emits green autofluorescence upon excitation with blue light. Studies on flavoprotein fluorescence (FPF) imaging have demonstrated that changes in the FPF in response to sensory stimulation are much faster and more localized compared to those in the cerebral vascular responses [7]. Furthermore, measurement of the FPF is more stable than that of the NADH fluorescence response [6]. FPF has been applied to functional imaging in the sensorimotor cortex [7], cerebellar cortex [6], auditory cortex [9], and visual cortex [10, 4] in rodents and cats.

K. Sakatani (✉)
Division of Optical Brain Engineering, Department of Neurological Surgery; Division of Applied System Neuroscience, Department of Advanced Medical Science, Nihon University School of Medicine, Tokyo, 173-8610, Japan
e-mail: sakatani@med.nihon-u.ac.jp

E. Takahashi, D.F. Bruley (eds.), *Oxygen Transport to Tissue XXXI*, Advances in Experimental Medicine and Biology 662,
DOI 10.1007/978-1-4419-1241-1_13,

However, it is not yet clear how cerebral ischemia affects the fluorescence; previous functional studies using the FPF have been conducted under normal circulatory conditions [7, 6, 9]. This issue is important for application of the FPF to research on functional reorganization after neuronal injury such as ischemic stroke. In the present study, we evaluated the effect of transient cerebral ischemia on the activity-dependent changes of FPF in the rat. We compared the changes of the FPF and somatosensory evoked potential (SEP) induced by transient cerebral ischemia.

2 Methods

2.1 Experimental Protocol

We employed adult male Fischer 344 rats (250 and 300 g, $n = 10$) anesthetized with 1.5% halothane. The right femoral artery was cannulated for recording of the arterial blood pressure and sampling of blood gases. The bilateral common carotid arteries were exposed, and closed with a tourniquet for transient forebrain ischemia. The rats then were fixed in a stereotaxic frame, and the right parieto-temporal bone was thinned (5 × 5 mm) over the sensorimotor cortex. Transient forebrain ischemia was induced by occlusion of the bilateral common carotid arteries for 60 min. The rectal temperature was maintained at about 37°C with an automatic heating pad. The arterial blood pressure (110 ± 8 mmHg, mean ± SD) remained stable throughout the experiments. The present animal experiments were performed carefully in accordance with the guiding principles for the care and use of laboratory animals approved by Nihon University School of Medicine.

2.2 Measurements of Flavoprotein Fluorescence

We recorded images of the green autofluorescence (barrier filter bandwidth, 500–550 nm) excited with blue light (excitation filter bandwidth, 450–490 nm) employing a cooled CCD camera system (AQUACOSMOS, Hamamatsu Photonics, Hamamatsu, Japan). The method of Britton Chance was referred to for measurement of the ratio of autofluorescence [3]. The left median nerve was stimulated with bipolar needle electrodes. The autofluorescence images (Fig. 1a) were analyzed by a pixel-by-pixel division to detect intrinsic signals, and the time course of the autofluorescence intensity was estimated (Fig. 1b). The autofluorescence responses reached a peak at 0.8–1.0 s after the stimulus onset, while the hemodynamic responses reached a peak at 2.0–2.5 s after the stimulus onset.

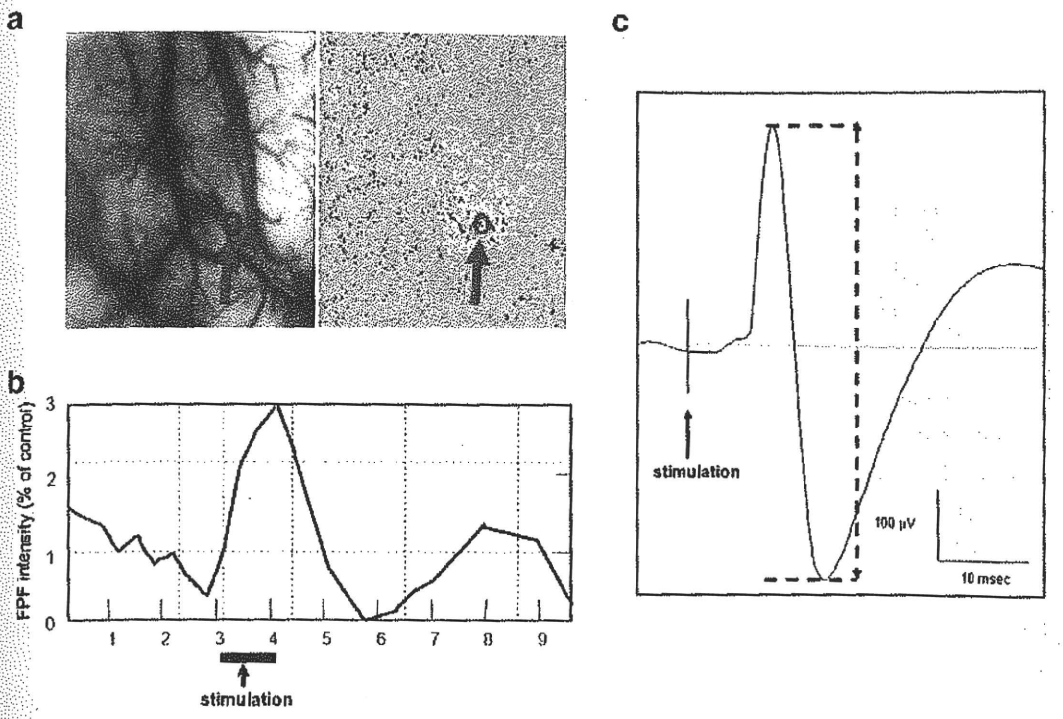

Fig. 1 **a**: Anatomical image of the recording area (*left*) and pseudo-color image of FPF changes during activation (*right*). **b**: Time course of the FPF intensity (*pink circle* in **a**) during activation. The ordinate indicates % change of FPF intensity. The thick horizontal bar indicates the period of electrical stimulation (1 s). **c**: Typical example of the SEP. The peak-to-peak amplitude was measured (*dotted lines*).

2.3 *Measurements of SEP*

We recorded the SEP with a Ag/AgCl ball electrode positioned at the forelimb area in the right sensorimotor cortex during left median nerve stimulation. A reference electrode was attached to the surrounding muscles and the ground lead was inserted in the right hind limb. The electrical stimulation was provided by a stimulator (SYNAX 2100, NEC), and 50 responses were averaged with a bandpass filter (10–1000 Hz). The amplitudes were measured peak-to-peak using the primary cortical response (Fig. 1c).

2.4 *Data Analysis*

Changes in SEP amplitude and FPF intensity were expressed as percentages of the responses under non-ischemic conditions (i.e. % SEP amplitude and % FPF intensity). Changes in regional cerebral blood flow (rCBF) caused by transient cerebral ischemia were measured with a laser-Doppler flowmeter (OMEGA-FLO FLO-N1, Omegawave). Changes in rCBF were expressed as a percentage of the non-ischemic baseline (i.e. % rCBF). Statistical analysis was performed

by means of an unpaired Student's *t*-test for comparisons involving the two ischemia models.

3 Results

Initially, we evaluated the frequency responses and intensity responses of the FPF and SEP under non-ischemic conditions ($n = 5$). Maximal SEP amplitude was observed at 0.5 Hz, and decreased with increase of the stimulus frequency. In contrast, the intensity of the FPF increased in association with increase of the stimulus frequency, and attained maximal intensity at 50 Hz (Fig. 2a). The FPF intensities and SEP amplitudes reached plateau levels at a stimulus intensity of over 4 mA (Fig. 2b). Based on these findings, we carried out ischemia-reperfusion experiments using supramaximal stimulation.

Occlusion of the bilateral common carotid arteries decreased the rCBF to $15.8 \pm 3.8\%$ of the controls. After reperfusion, the rCBF gradually recovered to $85.2 \pm 15.1\%$ of the controls at 90 min after reperfusion.

Figure 3a compares the changes in SEP and FPF during transient forebrain ischemia. The SEP and FPF disappeared rapidly after occlusion of the bilateral common carotid arteries. After reperfusion, the SEP and FPF gradually recovered; however, the recovery rates of the FPF were significantly faster than those of the SEP at 15 min ($p < 0.05$) and 30 min ($p < 0.01$) after reperfusion (Fig. 3b).

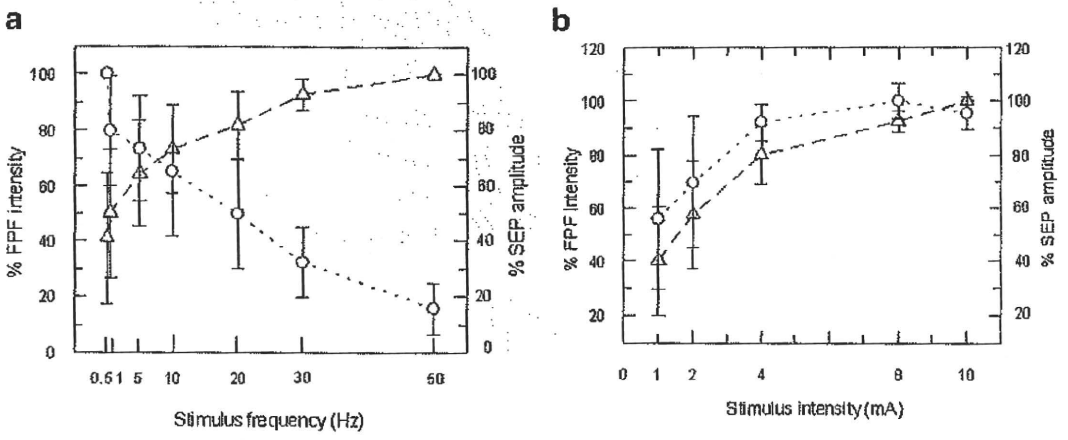

Fig. 2 **a**: Frequency responses of the FPF intensity and SEP amplitude. The ordinates indicate % changes of the maximal responses of the FPF intensity (*left*) and SEP amplitude (*right*), while the abscissa indicates the stimulus frequency (Hz). Open circles (○, n = 5) indicate the mean value of the % SEP amplitude; open triangles (△, n = 5) indicate the mean value of the % FPF intensity. **b**: Stimulus intensity responses of the FPF intensity and SEP amplitude. The ordinates indicate % changes of the maximal responses of the FPF intensity (*left*) and SEP amplitude (*right*), while the abscissa indicates the stimulus intensity (mA)

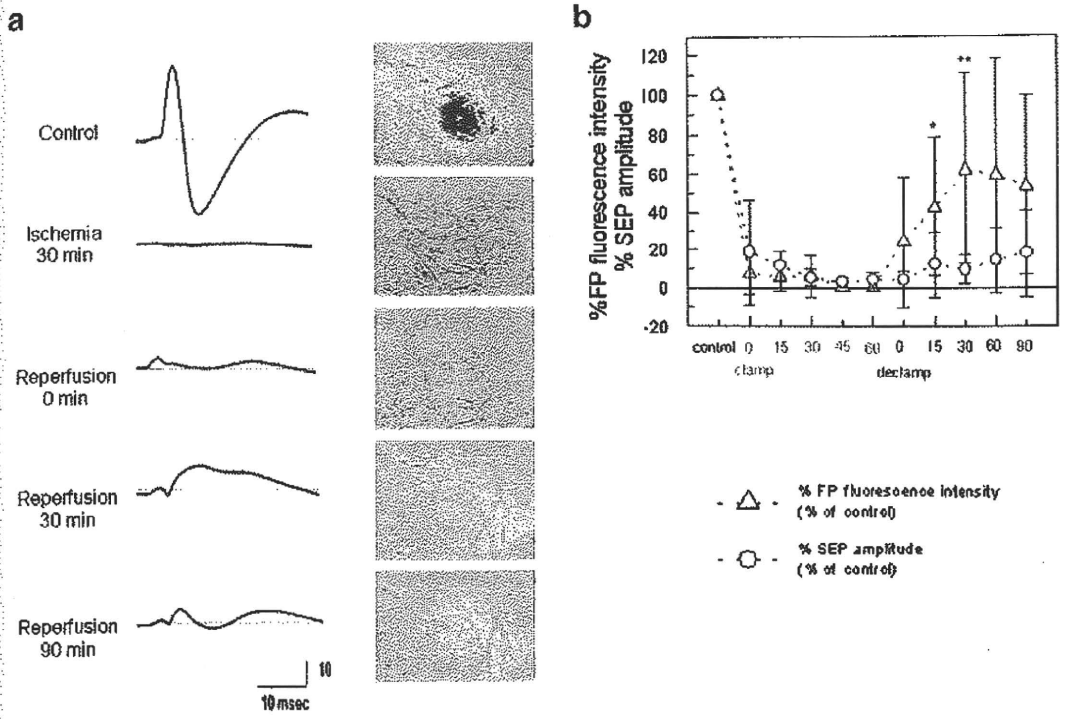

Fig. 3 a: Changes of SEP amplitude and FPF intensity during cerebral ischemia and after reperfusion in the 60-min ischemia model. **b**: There were significant differences in recovery rate between the SEP amplitude and FPF intensity at 15 and 30 min after reperfusion (*$p <$ 0.05, **$p < 0.01$)

4 Discussion

The present study demonstrated that the recovery rate of the SEP amplitude was significantly slower than that of the FPF after transient forebrain ischemia for 60 min. These findings indicate that transient cerebral ischemia affects the relation between activity-dependent changes of the FPF and the electrical activity.

Although the physiological mechanism of the dissociation in recovery rates between the FPF and SEP is not yet clear, FPF signal from astrocytes may play a role in the higher recovery rate of the FPF after reperfusion. Several reports have proposed that astrocytes play an important role in the active control of neuronal activity and synaptic neurotransmission [1, 5]. Astrocytes respond to neuronal activity with an increase of their internal Ca^{2+}, which triggers the release of chemical transmitters from the astrocytes themselves and, in turn, causes feedback regulation of the neuronal activity and synaptic strength. Such activity of astrocytes during neuronal activity could induce oxidation of flavoprotein in the electron transfer system, leading to emission of autofluorescence similar to that of neurons. Indeed, it has been demonstrated that the autofluorescence intensity was significantly decreased by the blocking of glial activity [2]. It should be noted that astrocytes are relatively resistant to ischemia as

compared to neurons [8]. These observations suggest that the FPF signal from astrocytes might be involved in the greater recovery of the FPF response after reperfusion in the 60-min ischemia model.

Conclusion: The present findings indicate that activity-dependent changes of the FPF do not necessarily correlate with the electrical activity after transient cerebral ischemia. The following mechanisms are suggested for the dissociation in recovery rates of the FPF and SEP after reperfusion. First, the FPF signal from astrocytes may contribute to the higher recovery rate of the FPF. Second, there are differences in ischemic tolerance between the cortical layers which generate FPF and SEP signals; the second and third layers which generate the FPF are more resistant to ischemia than the fourth layer which generates the SEP.

References

1. Araque A, Parpura V, Sanzgiri RP et al. (1998) Glutamate-dependent astrocyte modulation of synaptic transmission between cultured hippocampal neurons. Eur J Neurosci 10:2129–2142.
2. Buchheim K, Wessel O, Siegmund H et al. (2005) Processes and components participating in the generation of intrinsic optical signal changes in vitro. Eur J Neurosci 22:125–132.
3. Chance B, Legallais V (1963) A spectrofluorometer for recording of intracellular oxidation-reduction states. IEEE Trans Biomed Eng 10:40–47.
4. Husson TR, Mallik AK, Zhang JX et al. (2007) Functional imaging of primary visual cortex using flavoprotein autofluorescence. J Neurosci 27:8665–8675
5. Koizumi S, Saito Y, Nakazawa K et al. (2002) Spatial and temporal aspects of Ca^{2+} signaling mediated by P2Y receptors in cultured rat hippocampal astrocytes. Life Sci 72:431–442.
6. Reinert KC, Dunbar RL, Gao W et al. (2004) Flavoprotein autofluorescence imaging of neuronal activation in the cerebellar cortex in vivo. J Neurophysiol 92:199–211.
7. Shibuki K, Hishida R, Murakami H et al. (2003) Dynamic imaging of somatosensory cortical activity in the rat visualized by flavoprotein autofluorescence. J Physiol 549:919–927.
8. Siesjö BK (1988) Mechanisms of ischemic brain damage. Crit Care Med 16:954–963.
9. Takahashi K, Hishida R, Kubota Y et al. (2006) Transcranial fluorescence imaging of auditory cortical plasticity regulated by acoustic environments in mice. Eur J Neurosci 23:1365–1376.
10. Tohmi M, Kitaura H, Komagata S et al (2006) Enduring critical period plasticity visualized by transcranial flavoprotein imaging in mouse primary visual cortex. J Neurosci 26:11775–11785.

EJN fens EUROPEAN JOURNAL OF NEUROSCIENCE

European Journal of Neuroscience, Vol. 32, pp. 1145–1151, 2010 doi:10.1111/j.1460-9568.2010.07412.x

DEEP BRAIN STIMULATION

Deep brain stimulation for the treatment of vegetative state

Takamitsu Yamamoto,[1] Yoichi Katayama,[2] Kazutaka Kobayashi,[1] Hideki Oshima,[2] Chikashi Fukaya[1] and Takashi Tsubokawa[2]

[1]Division of Applied System Neuroscience, Department of Advanced Medical Science, Nihon University School of Medicine, 30-1 Ohyaguchi Kamimachi, Itabashi-ku, Tokyo 173-8610, Japan

[2]Department of Neurological Surgery, Nihon University School of Medicine, Tokyo 173-8610, Japan

Keywords: CM-pf complex, deep brain stimulation, mesencephalic reticular formation, minimally conscious state, spinal cord stimulation, vegetative state

Abstract

One hundred and seven patients in vegetative state (VS) were evaluated neurologically and electrophysiologically over 3 months (90 days) after the onset of brain injury. Among these patients, 21 were treated with deep brain stimulation (DBS). The stimulation sites were the mesencephalic reticular formation (two patients) and centromedian–parafascicularis nucleus complex (19 cases). Eight of the patients recovered from VS and were able to obey verbal commands at 13 and 10 months in the case of head trauma and at 19, 14, 13, 12, 12 and 8 months in the case of vascular disease after comatose brain injury, and no patients without DBS recovered from VS spontaneously within 24 months after brain injury. The eight patients who recovered from VS showed desynchronization on continuous EEG frequency analysis. The Vth wave of the auditory brainstem response and N20 of the somatosensory evoked potential could be recorded, although with a prolonged latency, and the pain-related P250 was recorded with an amplitude of > 7 μV. Sixteen (14.9%) of the 107 VS patients satisfied these criteria in our electrophysiological evaluation, 10 of whom were treated with DBS and six of whom were not treated with DBS. In these 16 patients, the recovery rate from VS was different between the DBS therapy group and the no DBS therapy group ($P < 0.01$, Fisher's exact probability test) These findings indicate that DBS may be useful for the recovery of patients from VS if the candidates are selected on the basis of electrophysiological criteria.

Introduction

On the basis of the results of lesioning and local stimulation, Moruzzi & Magoun (1949) proposed the concept of an ascending reticular activating system. Later anatomical studies revealed that widespread projection systems that originate from the brainstem pass through these areas, innervate wide areas of the cerebral cortex, and play an important role in this ascending reticular activating system (Kimura & Maeda, 1982; Vincent *et al.*, 1986; Aghajania & Vanderman, 1982; Kayama & Ogawa 1987). However, their findings and concept (Moruzzi & Magoun 1949) are quite reasonable, because a very strong arousal response can be induced by stimulating these areas even in humans (Tsubokawa *et al.*, 1990b; Katayama *et al.*, 1991). Temporary deep brain stimulation (DBS) for the treatment of long-term comatose-state patients was first reported by Hassler *et al.* (1969), and then by Strum *et al.* (1979). Hassler *et al.* (1969) stimulated the basal part of the pallidum and basal portion of the lateropolar nucleus of the thalamus, and observed a very strong arousal response. They were able to continue the stimulation for only 19 days, and no signs of awareness were observed in their patient. A chronic implantation system for DBS has recently become available for clinical use, and was clinically applied for the first time for the treatment of pain (Hosobuchi *et al.*, 1973; Adams *et al.* 1974; Richardson & Akil, 1977). On the basis of this DBS application, Tsubokawa *et al.* (1990b) and Chohadon & Richer (1993) reported on chronic DBS for vegetative-state (VS) patients.

The term persistent vegetative state (PVS) was first proposed by Jennett & Plum (1972), and was described as wakefulness without awareness. The Multi-Society Task Force on PVS (1994a,b) summarized the medical aspects of PVS as follows: VS is a clinical condition of complete unawareness of the self and the environment, accompanied by sleep–wake cycles, with either complete or partial preservation of hypothalamic and brainstem autonomic function. In addition, patients in a PVS show no evidence of sustained, reproducible, purposeful or voluntary behavioral responses to visual, auditory, tactile or noxious stimuli, show no evidence of language comprehension or expression, have bowel and bladder incontinence, and have variably preserved cranial-nerve and spinal reflexes.

In accordance with the above description of VS, we selected 107 VS patients who had remained in VS for > 3 months, and we evaluated these VS patients neurologically and electrophysiologically at 3–4 months after the onset of brain injury. Among these patients, 21 were treated with DBS (Fig. 1). At the start of DBS, we applied DBS to all the patients whose family could understand and agree with our DBS protocol. On the basis of electrophysiological evaluation and results of DBS in the initial VS patients, we established electrophysiological indication criteria for this DBS therapy. Thereafter, we applied DBS in accordance with the indication criteria as much as

Correspondence: Takamitsu Yamamoto, MD, PhD, as above.
E-mail: nusmyama@med.nihon-u.ac.jp

Received 13 March 2010, revised 20 July 2010, accepted 21 July 2010

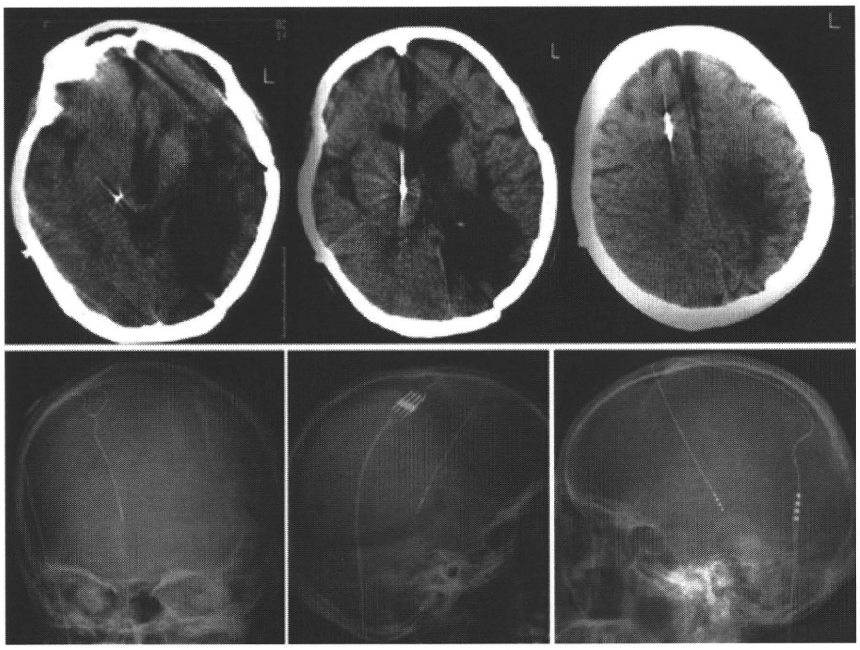

FIG. 1. Deep brain stimulation for treatment of a VS patient. The stimulating electrode was implanted for CM-pf stimulation. Computerized tomography (upper) and radiography (lower left and middle) show the trajectory and location of the old type of DBS electrode. Lower right indicates the present DBS electrode.

possible. Patients who qualified for inclusion on the basis of the indication criteria but whose family did not agree with our DBS therapy did not receive DBS. We followed up 21 patients for a minimum of 10 years (or until death), and assessed the long-term consciousness recovery of VS patients treated with DBS (Yamamoto *et al.*, 2002, 2003).

Materials and methods

Patients in VS treated with DBS

All the 21 patients who were treated with chronic DBS had been in a condition that satisfied the criteria for the diagnosis of VS outlined by the The Multi-Society Task Force on PVS (1994a), for at least 3 months prior to undergoing electrophysiological evaluation. The start of DBS was from 4 to 8 months after the onset of comatose brain injury. These patients were followed up until they deceased or for a minimum of 10 years after DBS. Most of these patients treated with DBS were followed up in general hospitals in our country, as were our other VS patients without DBS. After DBS, we evaluated neurological changes and also whether they showed any consistent and clearly discernible behavioral evidence of consciousness every month for 1 year, and twice a year in the following years. Their ages ranged from 19 to 75 (mean 43 ± 20.1) years old. The causes of the initial coma were head injury (nine patients), cerebrovascular accident (nine patients) and anoxic brain (three patients).

Patients in VS without DBS

Eighty-six patients who were not treated with chronic DBS had been in a condition that satisfied the criteria for the diagnosis of VS outlined by the The Multi-Society Task Force on PVS (1994a,b), for at least 3 months prior to electrophysiological classification. In Japan, everyone is covered by the national health insurance, so that all these VS patients were treated similarly to the DBS patients except for the DBS treatment. The ages ranged from 18 to 86 (mean 41 ± 18.3) years old. The causes of the initial coma were cerebrovascular accident (40 patients), anoxic brain (28 patients) and head injury (18 patients). Among these patients, six who were candidates for DBS in accordance with our electrophysiological criteria for DBS had families who disagreed with our DBS protocol. The causes of initial coma of these six patients were cerebrovascular accident (three patients) and head injury (three patients), and their ages ranged from 26 to 66 (mean 45 ± 17.4) years old. All the patients' families agreed to contact us and report whether their respective patients began to show any consistent and clearly discernible behavioral evidence of consciousness. We also made contact with the patients' families and patients' transferred hospitals at 6, 12, 18 and 24 months after the elecrophysiological evaluation.

Electrophysiological evaluation of VS

At from 3–4 months after the onset of the comatose state, neurological and neurophysiological evaluations were carried out (Tsubokawa *et al.*, 1990a; Yamamoto *et al.*, 2002, 2003). The neurophysiological evaluations included assessments of the auditory brainstem response (ABR), somatosensory evoked potential (SEP), pain-related P250, and continuous EEG frequency analysis expressed as a compressed spectral array (CSA). EEG recording was carried out at the bedside with a monopolar lead, and electrodes were placed in the parietal area and earlobe on both sides. EEG recording was displayed as a CSA for EEG frequency analysis, employing a fast Fourier transform. The CSA was classified into three types similar to those used in the study by Bricolo *et al.* (1978) as follows: (i) slow monotonous spectrograms whose main feature is the presence of pronounced peaks in the low-frequency band, recurring monotonically in separate samples; (ii) changeable spectrograms whose spectra are characterized by constant and predominant activities at low frequencies associated with variously pronounced and organized peaks at alpha or higher

frequencies and (iii) borderline spectrograms whose main feature is that most of the power is centered in the alpha frequency band and the peaks show an extremely regular and stable frequency (Fig. 2A). We further classified the changeable spectrograms into three types because there were clearly different patterns among such spectrograms (Tsubokawa *et al.*, 1990a), as follows. (i) No desynchronization pattern: changes in peak frequency are present only at alpha and lower frequencies, but not at higher frequencies. (ii) Slight desynchronization pattern: desynchronization is present but does not appear frequently; the duration is short, being < 10% of the time course, and the power of a high frequency is low. (iii) Desynchronization pattern: desynchronization (a change to low amplitude and high frequency) appears frequently, and the increase in high-frequency power is clear at desynchronization (Fig. 2B).

ABR was recorded by placing needle electrodes on the vertex (Cz), earlobes and forehead (ground). The bandpass filtering was set from 10 Hz to 3 KHz. Earphones were used to present binaural click stimuli at 90 dB HL at a rate of 10 Hz. Each trial consisted of 2048 responses. The SEP was recorded from a needle electrode placed over the primary cortical somatosensory regions on the head, with the reference electrode placed on the earlobe. The bandpass filtering was set from 0.5 Hz to 3 KHz. The pain-related P250 (Katayama *et al.*, 1985) was recorded from the vertex in response to a train of electrical shocks applied at random to the finger pad. For painful electrical skin stimuli, constant current pulses of 0.5 ms duration were applied at a repetition rate of 500 Hz for 50 ms. The intensity of the stimulus was adjusted to a level that produced a withdrawal flexion reflex. Recording electrodes were referred to the earlobe and placed on the vertex and hand region of the somatosensory cortex. Grounding was to the other earlobe or the wrist. Signals were amplified with the bandpass filtering from 0.1 to 6000 Hz and were averaged for 16 sweeps with a signal processor (Fig. 3).

DBS for VS

Chronic DBS was carried out using a chronically implanted flexible wire electrode inserted by stereotactic surgery under local anesthesia (Tsubokawa *et al.*, 1990a,b; Yamamoto *et al.*, 2004). As target points

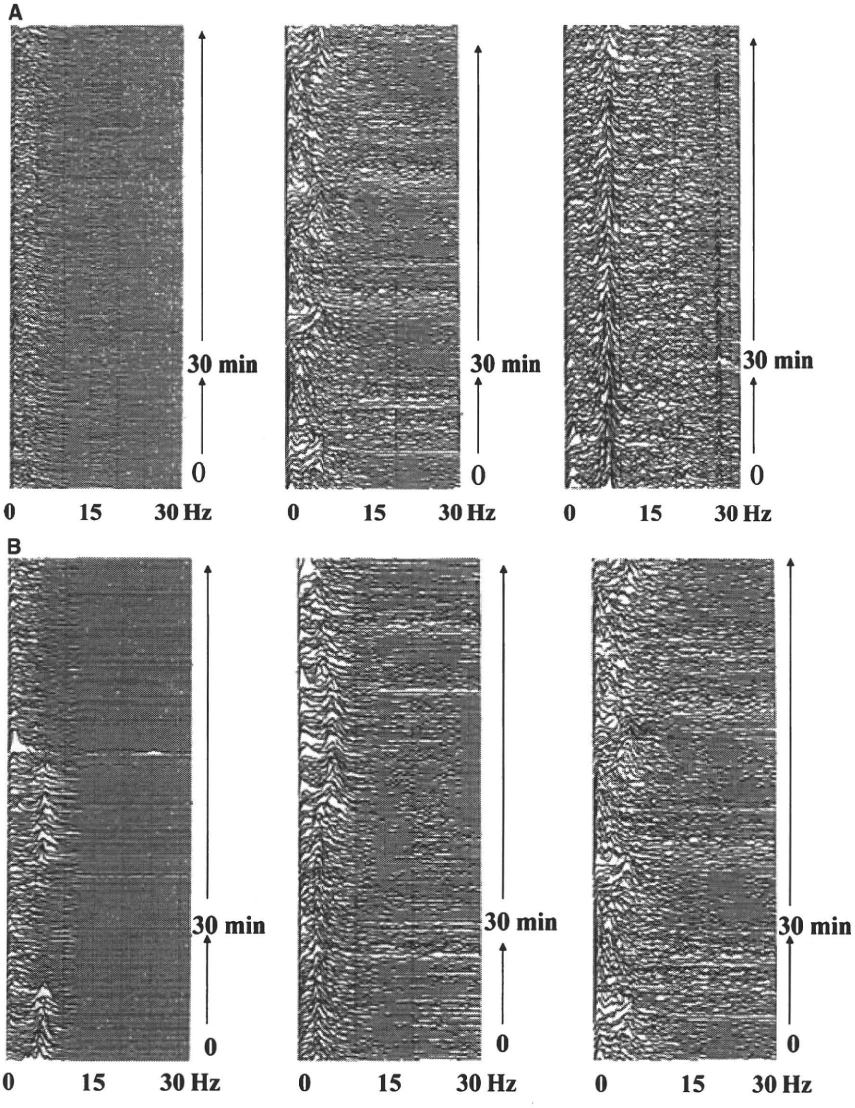

FIG. 2. (A) Three types of compressed spectral array of continuous EEG frequency analysis of VS patients. Slow monotonous spectrum (left), changeable spectrum (middle), and borderline spectrum (right). (B) Changeable spectrograms were classified into no desynchronization pattern (left), slight desynchronization pattern (middle) and desynchronization pattern (right).

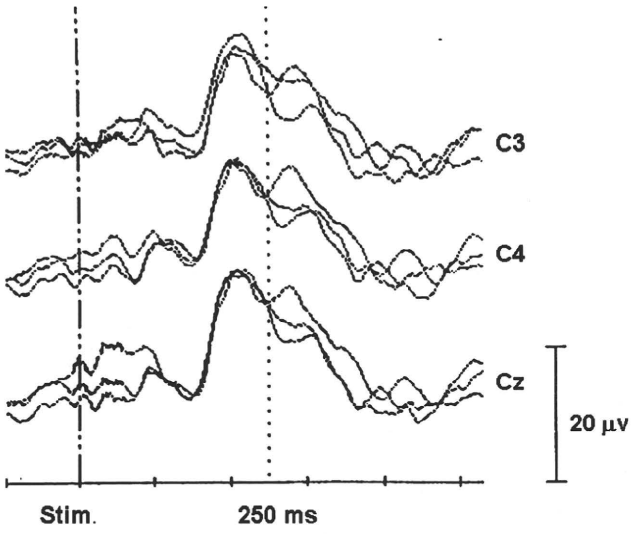

FIG. 3. Pain-related P250 recording in a VS patient. C3, C4 and CZ indicate the locations of recording electrodes.

for chronic DBS, the mesencephalic reticular formation (MRF; two patients) and centromedian–parafascicularis nucleus (CM-pf) complex (19 patients) were selected. Stimulation was applied every 2–3 h during the daytime, and was continued for 30 min at a time. The stimulation frequency was mostly fixed at 25 Hz, and the stimulation intensity was determined depending on the response of each patient, being slightly higher than the threshold for inducing an arousal response. To apply chronic DBS, we first used a chronically implanted flexible wire electrode (model 3380; Medtronic Inc., Minneapolis, MN, USA) and a transmitter–receiver system (models 3470 and 3425; Medtronic) at the time when we started this therapy. After that, we used more suitable electrodes (model 3387; Medtronic) for DBS and an implantable pulse generator (model 7426; Medtronic Inc.), which are now widely used for various DBS therapies. The target point in the MRF was the nucleus cuneiformis, which is located in the dorsal part of the nucleus ruber and the ventral part of the deep layer of the superior colliculus. The CM-pf complex was selected as the stimulating point in the nonspecific thalamic nucleus. We followed up the 21 patients for > 10 years and assessed their consciousness and functional recovery. All the patients' families provided written informed consent for this procedure. This study was approved by the Committee for Clinical Trials and Research on Humans of our university and conformed to the principles outlined in the Declaration of Helsinki.

Statistical analysis

The resting brain function was different for each VS patient. There were 16 patients who were included in our electrophysiological indication criteria for DBS. In these 16 patients, the recovery rate from VS was compared between the DBS therapy group and the no-DBS therapy group using Fisher's exact probability test.

Results

Stimulation-induced phenomena

The features of the stimulation at the given targets were such that the patients presented strong arousal responses that were observed immediately at the start of stimulation. The patients opened their eyes with dilated pupils, the mouth sometimes also opened widely with meaningless vocalizations, and a slight increase in systemic blood pressure was observed during the stimulation. Moreover, some patients revealed slight movements of the extremities. During the MRF or CM-pf complex stimulation, the regional (r-) cerebral blood flow (CBF; r-CBF) increased markedly (Fig. 4). The stimulation of both the MRF and CM-pf complex induced a strong arousal response and the same phenomena. On the basis of these findings we mainly carried out stimulation of the CM-pf complex as it is the source of the wide-spreading projection system to the cerebral cortex and electrode implantation is safer.

Long-term effect of DBS for VS

Eight of the 21 patients recovered from VS and could communicate with some speech or other responses, but needed some assistance with their everyday life in bed. Even after long-term rehabilitation, their bedridden status remained unchanged except for one patient. These eight patients recovered from VS, but they remained in the severe disability condition based on the Glasgow Outcome Scale. The other 13 patients were unable to communicate at all and either deceased or failed to recover from VS within a minimum of 10 years. The recovery from VS of these eight patients occurred between 4 and 12 months after the start of DBS. On the basis of these results, we consider that it is necessary to continue DBS for at least 12 months or until recovery from VS to assess the efficacy of DBS. After recovering from VS, DBS was no longer necessary because their consciousness level did not change even if DBS was stopped. In the eight patients who recovered from VS following DBS, the Vth wave of the ABR was recorded,

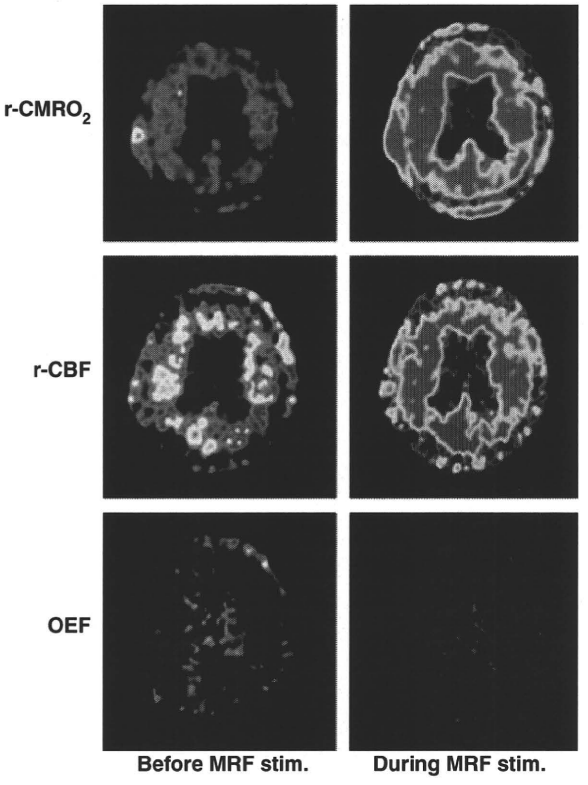

FIG. 4. Changes in r-CBF, regional cerebral metabolic rate of oxygen (r-CMRO2) and oxygen extraction fraction (OEF) before and during stimulation of MRF in a VS patient. r-CBF and r-CMRO2 increased in the whole brain without changing OEF.

although with a prolonged latency, N20 of the SEP was recorded from at least one side, continuous EEG frequency analysis revealed a desynchronization pattern or slight desynchronization pattern and pain-related P250 was recorded with an amplitude of > 7 μV.

Such electrophysiological findings on patients in VS were seen in 16 (14.9%) of the 107 VS patients, and 10 of the 21 patients treated with DBS satisfied these criteria. On the basis of the results of the initial DBS, we established the electrophysiological indication criteria for DBS. That is the reason why 10 of the 21 DBS patients satisfied the indication criteria, although only 14.9% of the 107 VS patients satisfied the electrophysiological indication criteria.

In accordance with the electrophysiological indication criteria, eight of the 10 VS patients treated with DBS recovered from VS and were able to obey verbal orders. On the other hand, the other six patients who satisfied these indication criteria but were not subjected to DBS did not recover from VS spontaneously within 2 years. In the 16 patients who satisfied the electrophysiological indication criteria, the recovery rate from VS was different between the DBS therapy group and the no-DBS therapy group ($P < 0.01$, Fisher's exact probability test). Among the patients who recovered from VS, the causes of the initial coma were head injury (two patients) and cerebrovascular accident (six patients). The above eight patients remained bedridden even after recovering from VS, and only one patient recovered from the bedridden state later. These results indicate that DBS is effective for the recovery of consciousness in some VS patients, but physical and motor functional recovery is difficult in patients who remain in VS for a long period (Fig. 5).

Discussion

In VS patients, cortical brain functions are more disturbed than brainstem functions, and it has been reported that thalamocortical relations and the relationship between the brainstem and cerebral cortex are important for maintaining consciousness (Dempsey & Morison, 1942; Moruzzi & Magoun, 1949; Starzl *et al.*, 1951; Dickman, 1968). Electrical stimulation of the CM-pf complex can induce incremental recruiting and augmenting responses in EEG in the case of low-frequency stimulation and EEG desynchronization in the case of high-frequency stimulation (Jasper *et al.*, 1955; Weinberger *et al.* 1965; Sasaki *et al.*, 1970). We therefore selected the CM-pf complex as a target for the treatment of VS. We unilaterally stimulated MRF or CM-pf complex, and selected the

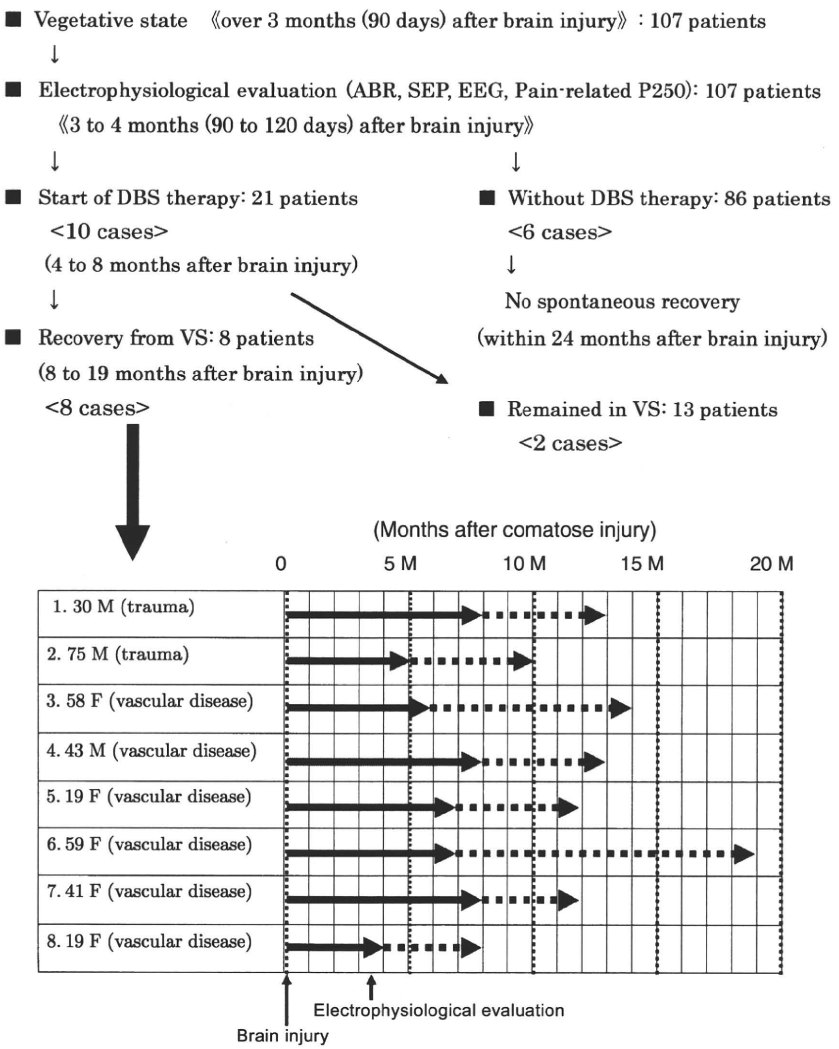

FIG. 5. Long term follow-up results of VS patients evaluated electrophysiologically at > 3 months (90 days) after comatose brain injury. The numbers in < > indicate the number of patients who satisfied our electrophysiological indication criteria. In the lower chart, the solid arrow indicates the duration of VS before DBS, and the dotted arrow indicates the duration of DBS until recovery from VS.